FULL PAPER

**ADVANCED
THEORY AND
SIMULATIONS**

Stress Deflection

www.advtheorysimul.com

A Natural Stress Deflector on the Head? Mechanical and Functional Evaluation of the Woodpecker Skull Bones

Jae-Young Jung,* Andrei Pissarenko, Adwait A. Trikanad, David Restrepo, Frances Y. Su, Andrew Marquez, Damian Gonzalez, Steven E. Naleway, Pablo Zavattieri, and Joanna McKittrick

The brain is one of the most important and complicated organs, but it is delicate and therefore needs to be protected from external forces. This makes the pecking behavior of the Woodpecker so impressive, as they are not known to sustain any brain injury due to their anatomical adaptations (a specialized beak, skull bone, and hyoid bone). However, the relationship between the morphology of the woodpecker head and its mechanical function against damage from daily pecking habits remains an open question. Aided by recent technical advancements, these questions can be explored by applying new materials science concepts of bioinspiration and bioexploration to identify adapted structures/materials in a design that results from millions of years of evolution. Two main features, including the beam-like bar structure of the jugal bone acting as a main stress deflector and the high natural frequency of the skull bone of woodpeckers can teach two lessons for potential materials development as well as engineering applications: protection of a delicate internal organ occurs by redirection of the main stress pathway and a large mismatch of the natural frequencies between the skull and brain avoids resonance and reduces the overall load experienced by the brain.

Dr. J.-Y. Jung, Dr. F. Y. Su, Prof. J. McKittrick
Materials Science and Engineering Program
University of California, San Diego
La Jolla, CA 92093, USA
E-mail: jyjung@ucsd.edu
A. Pissarenko, Dr. A. Marquez, D. Gonzalez, Prof. J. McKittrick
Department of Mechanical and Aerospace Engineering
University of California, San Diego
La Jolla, CA 92093, USA
A. A. Trikanad, Dr. D. Restrepo, Prof. P. Zavattieri
Lyles School of Civil Engineering
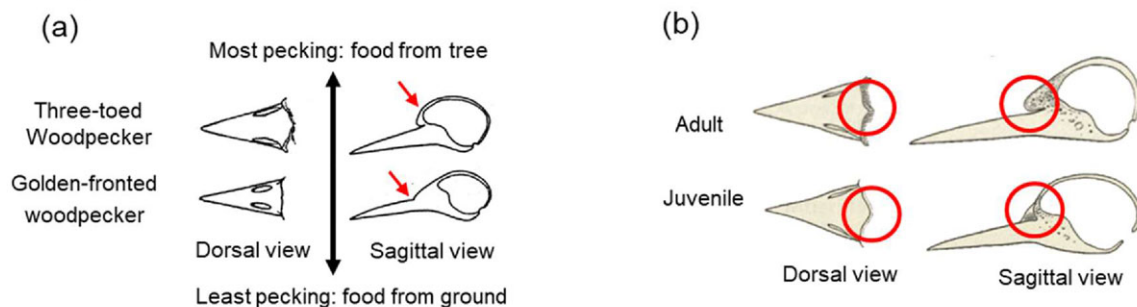Purdue University
West Lafayette, IN 47907, USA
Prof. D. Restrepo
Department of Mechanical Engineering
The University of Texas at San Antonio
San Antonio, TX 78249, USA
Prof. S. E. Naleway
Department of Mechanical Engineering
The University of Utah
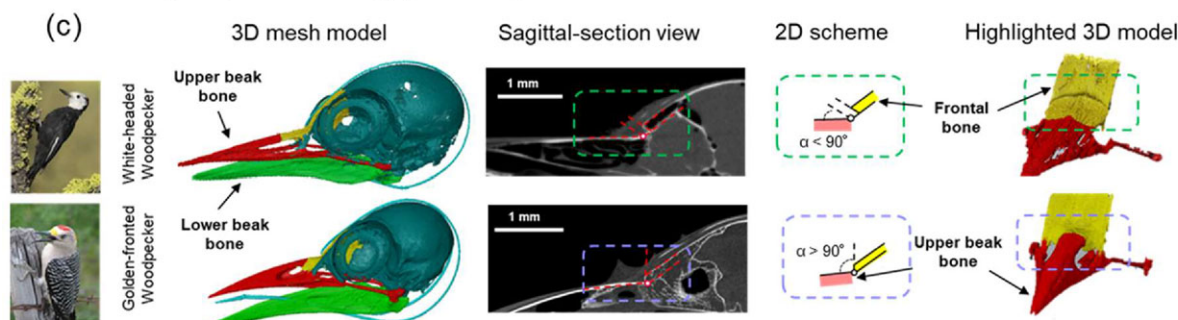Salt Lake City, UT 84112, USA

The ORCID identification number(s) for the author(s) of this article can be found under https://doi.org/10.1002/adts.201800152

DOI: 10.1002/adts.201800152

1. Introduction

Concussion is a form of mild traumatic brain injury (mTBI) caused by external mechanical forces. It is a common occurrence and happens frequently during contact sports (e.g., football, hockey) or from direct or sheer trauma that can occur during vehicle accidents, for example.[1] Repeated exposure to mTBI eventually causes chronic traumatic encephalopathy, a progressive degenerative disorder, resulting in symptoms such as memory loss, decline of executive function, depression, impulsivity, aggressiveness, and suicidal behavior.[2]

Woodpeckers peck at trees every day throughout their 15-year life span; however, amazingly, no evidence has been found of chronic TBI or concussion in their brains. Materials scientists and mechanical engineers have attempted to understand and identify key elements of the woodpecker's shock tolerance in terms of biomechanics. With impact conditions reaching decelerations up to 1200 g, 7 m s^{-1} of impact speed, and pecking rates around 20 Hz,[3] there are hypotheses stating that woodpeckers have evolved and adapted to absorb the impact energy at the moment of impact.[3a,4]

In terms of adaptation and evolution, Bock[4] pointed out that an adaptive beak shape and cranial kinesis (relative movement between the upper jaw and the skull) can explain the shock-absorbing mechanism. The author's hypothesis was inspired by an earlier finding made by Burt[5] that some woodpeckers that hammer more frequently than others present an anatomical adaptation on their skull bone, called the frontal overhang (shown in **Figure 1**a with red arrows). This finding was based on the foraging behavior associated with the main food sources as well as the development of birds (shown in Figure 1a,b), and this was the first report regarding a structural specialization on the skull bone.[6] Some suggested other features (e.g., a relatively short leg length and the variation of size of rib bones)[7] that might be related to pecking habits are described in detail in S1.1, Supporting Information.

Several researchers have collected data on the mechanical properties of the heads, and more particularly for the skull and beak bones. Gibson[8] described an allometry effect (implying that physical parameters, generally size and mass, scale with

ADVANCED
SCIENCE NEWS
www.advancedsciencenews.com

ADVANCED
THEORY AND
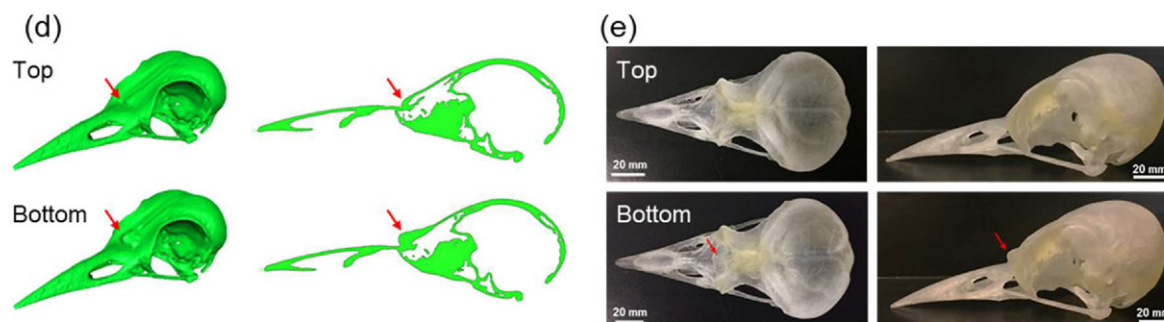**SIMULATIONS**
www.advtheorysimul.com

Figure 1. An example of how a biological observation becomes a scientific design and experiment. A representative anatomical adaption of the skull bone based on the relationship between food source and pecking behavior in woodpeckers, showing a) two representative species chosen from nine different woodpecker species reported by Burt[5] and highlighted by Bock[22] and b) the differences of the skull bone between the adult and juvenile birds. c) A comparison of different skull bone structures between a white-headed woodpecker and a golden-fronted woodpecker: (left to right) photographs of two woodpeckers, its 3D reconstructed model of the skull and beak bones from micro-computed tomography, 2D images of sagittal-section views, and simplified schemes of two adjacent bones (the frontal bone and upper beak bone), and highlighted 3D models. d) Two models of the skull bone for dynamic finite element analysis and frequency modal analysis: (top) the reconstructed original model, mimicking a golden-fronted woodpecker, and (bottom) the model with the artificial overhang, mimicking a white-headed woodpecker. The images on the right side are the view-cut sections along the sagittal plane. e) 3D printed skull models using a transparent material (the same dimensional order as Figure 1d).

certain properties or features) between the human and woodpecker heads in terms of a concussion limit and concluded that this scaling effect enables woodpeckers to avoid brain injury due to the relatively smaller size, the short duration of impact, and large contact area between the brain and the skull bone. This is the first comparative analysis considering the relative size of human and woodpeckers but the interspecies variation was not fully considered (e.g., the body masses of an ivory-billed woodpecker and a golden-fronted woodpecker are up to ≈570

and ≈90 g, respectively). Other mechanical analyses based on computational and experimental results are described in more detail in S1.2, Supporting Information, including: a simplified 2D finite elemental analysis (FEA) of the whole head impact,[9] the mechanical properties of the woodpecker hyoid bone,[10] some 3D FEA studies,[11] and biomimicking protection devices for microelectronics.[12] Recently, a comparative analysis of the skull bones of woodpeckers and chickens was reported,[13] illustrating that the skull bone of woodpeckers showed structural

differences such as a relatively small but uniform level of closed porosity, a higher degree of mineralization, and a higher cortical to skull bone ratio than those of chickens. Consequently, it was found that woodpeckers have stiffer bones than chickens, but also that the mechanical properties gradually decrease as one moves from the beak toward the skull, in a gradient fashion.

Regarding the relationship between the pecking habits and anatomical features, here it is hypothesized that the frontal overhang, as observed by Bock[14] and Burt,[5] is an evolutionary adaptation among certain species of woodpeckers that is directly correlated with their pecking habits. Therefore, we adopted a strategy to perform a comparative study based on function and morphology. According to Smith,[15] this approach includes the following steps: 1) an analysis of shape and behavior about a key element on the structural function and role in the natural environment of animals (shown in Figure 1a,b), 2) a phylogenetic analysis from the morphology (shown in Figure 1a and Figure S1, Supporting Information), 3) a selection of a valid model of function (Figure 1c), 4) building hypotheses about the relationship between function and structure, 5) expectations for morphological variance in terms of the model of function compared to knowledge of animal's behavioral differences, and 6) performing a test to validate the hypotheses with comparative analysis (across **Figures 2** and **3**).

Following the hypothesis formulated above, this study aims to confirm whether anatomical differences on the frontal bone in some species of woodpeckers present any mechanical advantage in relation to their reported behavioral/food habits.

A morphological comparative analysis (as shown in Figure 1c) shows different skull bone structures between two woodpeckers: a white-headed woodpecker (more frequent pecking) and a golden-fronted woodpecker (less pecking). In Figure 1c, each bone is shown with a different color. Note that the nasal-frontal hinge (yellow color) is generally a movable joint at the interface between the upper beak bone and the frontal bone, for common avian species, but most woodpeckers show prokinesis, meaning that the hinge is located between the frontal and nasal bones.[4,14] Based on the micro-computed tomography (μ-CT) results reported by Jung et al.,[13] as well as shown in Figure 1c in this paper, this hinge structure was completely fused to the frontal bone (in a male, adult specimen). Therefore, the nasal-frontal hinge, including the frontal overhang (yellow in Figure 1c) was not considered as a movable joint in our further mechanical analysis. A sagittal-section view of two woodpeckers showed an emphasis on the overhang structure by having a different angle between the frontal bone and the upper beak bone. The dotted lines with a red color were drawn along the upper edge of the upper beak bone and the frontal bone to represent the angle (α in Figure 1c) and shape in two dimensions. Those lines were copied and redrawn in 2D scheme images, where red represents the upper beak bone and yellow represents the frontal bone. The results show that for the white-headed woodpecker, the hinge on the upper beak bone does not intersect with the upper beak bone, and the hinge opening angle (α) is smaller than 90°, as shown by the two lines on Figure 1c. On the other hand, the upper beak bone and the frontal bone of the golden-fronted woodpecker intersect each other without any gap in between, this time with a larger hinge opening angle ($\alpha > 90°$), as illustrated by the single red line. When reconstructed and visualized in three dimensions,

the differences become clearer: there is a shaded region near the interface between the upper beak bone and the frontal bone on the white-headed woodpecker, whereas the golden-fronted woodpecker has a smooth interface in the same region. From the μ-CT scan results (shown in Figure 1c, right), it is confirmed that there are structural differences of the skull bone of woodpeckers among different species, which can potentially be related to pecking habits and food sources (presented in Figure S1, Supporting Information). Based on the findings that some woodpeckers indeed possess a frontal overhang structure while others do not, a further identification of the structural role of the frontal overhang needs to be performed.
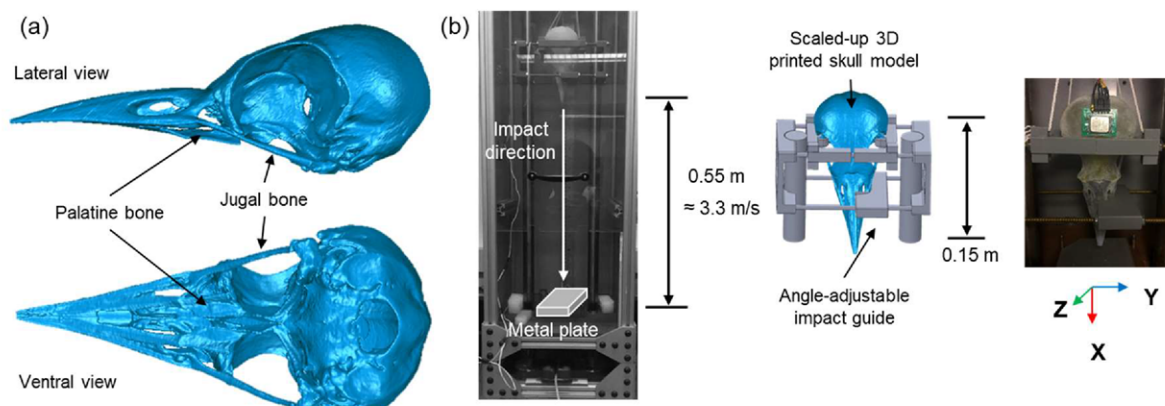
2. Experimental and Computational Approach

To simplify and facilitate the comparison between the overhang and non-overhang species, 3D models of solely the golden-fronted woodpecker were generated from the μ-CT scans, as shown in Figure 1d (top). On one model, an artificial overhang was added with an increased volume on the frontal bone, mimicking the frontal overhang structure found in the white-headed woodpecker (shown in Figure 1d, bottom). View-cut sections were made at the centroid and the pseudo-symmetry plane to highlight the morphological changes between the two models. Then, 3D printed skull models (scaled up by a factor of three to facilitate experimental procedures) were obtained as shown in Figure 1e (top: a no overhang model, bottom: an overhang model).

To test our hypothesis that the skull bone of woodpeckers has adapted to avoid brain injury, impact testing of the 3D printed skull models was implemented so as to best reproduce the pecking conditions of woodpeckers. A wooden plate was first considered for a realistic pecking condition with an impact speed of 7 m s^{-1}. However, the plates would absorb most of the impact energy showing dents on their surface while the 3D skull models would not show any sign of failure or damage. In contrast, a worst-case scenario was implemented by impacting against a metal plate. An experimental setup to obtain the accelerations of the skull bone near the brain in three axes using a customized drop-weight test tower is presented in Figure 2a. A maximum impact speed of 3.3 m s^{-1} was achieved from the maximum height with a customized, 3D printed impact guide, adjusting and holding the angle of impact of the woodpecker skull (Figure 2b,c). A three-axis accelerometer was attached to the skull model to measure the accelerations at the moment of impact (Figure 2b, right).

A modal analysis was performed in Abaqus/Standard to characterize the frequency response of the woodpecker under free vibration response. Some representative nodes on the main pathway of stress waves are identified as shown in Figure 2c: two points along the dorsal line (node 1 and node 2) as well as two other points along the ventral line (node 3 and node 4). Note that the node 2 is at the identical location where the accelerometer was attached on the 3D printed skull model. Then, further validation of the modal analysis was performed using Abaqus/Explicit where a Ricker's pulse input, allowing a correlation between the propagation of stress waves in a time domain space and the principal frequencies that are excited during impact events in the woodpecker's skull. Ricker wavelets are widely used in seismic and vibrational studies because these can be uniquely specified

ADVANCED
SCIENCE NEWS
www.advancedsciencenews.com

ADVANCED
THEORY AND
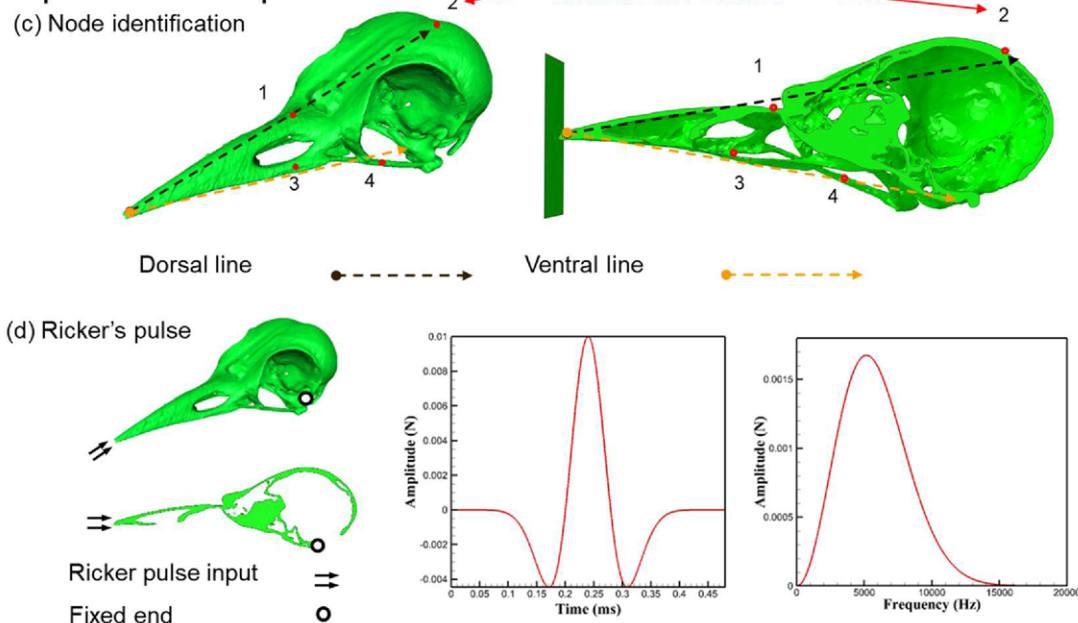SIMULATIONS
www.advtheorysimul.com

Figure 2. An illustration of experimental and computational test design of an impact test using 3D printed woodpecker skull models. a) Lateral (top) and ventral (bottom) views of the 3D reconstructed skull models with its anatomy. Each arrow indicates the palatine and jugal bone, respectively. b) A photo of an impact test drop tower (left), a CAD design of a custom-built 3D printed impact guide (middle), and a photo of 3D printed skull loaded on the tower with an impact guide with an attached accelerometer (right). The maximum drop height and impact speed were adjusted due to the height of the impact guide. c) Node identification of each region of interest, 1: the caudal end of the upper beak bone, 2: on the parietal bone near the brain (the accelerometer attached location), 3: on the palatine bone, and 4: on the jugal bone. d) Schematic illustration of the Ricker's pulse input and the fixed end location considered in the frequency modal analysis (left), in time (middle), and frequency domain (right).

with only a single parameter that corresponds to its peak frequency on the wavelet's frequency spectrum.[16]

3. Results and Discussions

From the experimental results, accelerations were measured in all three axes of the no overhang model at an impact speed of 3 m s^{-1} (Figure 3a). Note that the main impact direction is along the X-axis (red arrow). The first peak of the measured acceleration over time in the X-axis showed the highest value of acceleration (max 529 g) compared with other axes. The impact duration, corresponding to the width of the first peak, is approximately 1 ms. After a few minor fluctuations, the accelerations were dampened by less than a half at the second peak in the X-axis (190 g). For the Y-axis, which is an indication of the lateral movement of the skull model (left and right motion of the 3D printed model in Figure 3a), the acceleration peaks were much smaller than the X-axis. It means that the lateral displacement (and/or vibration) of the skull model is much
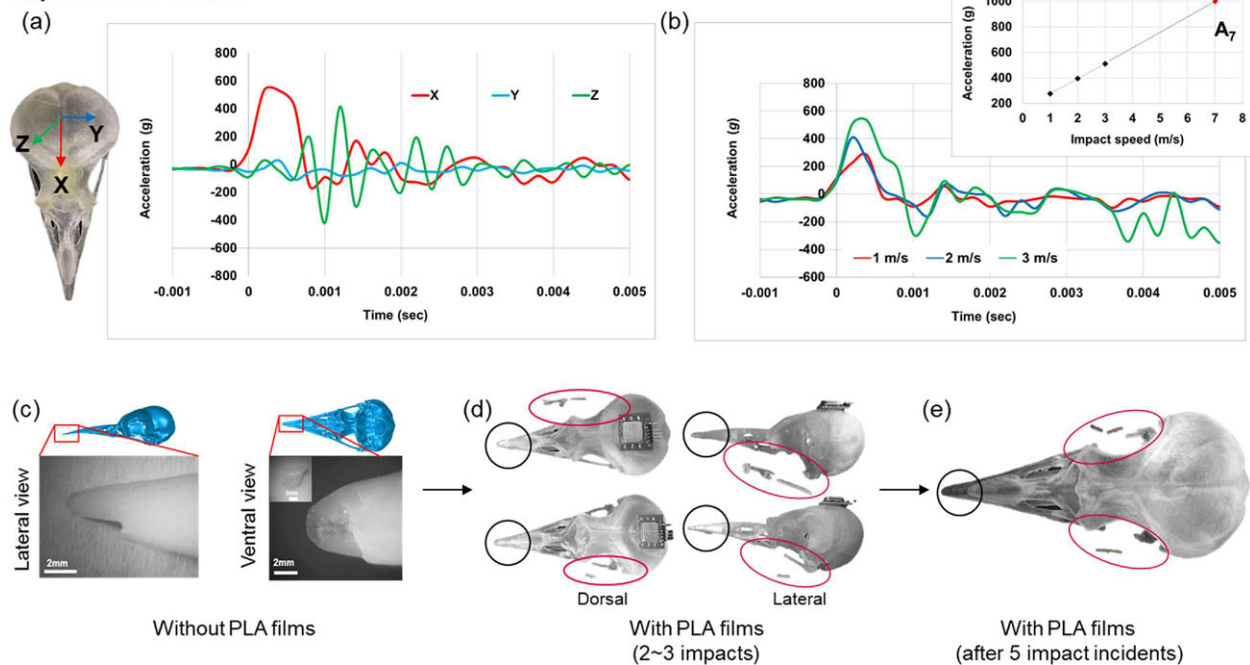
Experimental results

Figure 3. Experimental results of the impact testing with 3D printed skull models. a) Measured acceleration on the skull bone near the brain in an impact speed of 3 m s^{-1} for three-axes. b) The effect of different impact speeds at 1, 2, and 3 m s^{-1} on the accelerations at the X-axis. Note that an inset plot shows the linear regression line of acceleration at a 7 ms^{-1} (A$_7$). c) Photos of damaged skull models without the beak cover. d) After using a PLA wrap (black circles) to mimic the keratinized sheath in the beaks, the damages of the skull models were mainly found on the jugal bone after 2–3 times of impacts. e) After five times of impact incidents: only the jugal bones were damaged. Note that other structures remained intact.

smaller than the X-axis at the moment of impact. The maximum intensity of accelerations on the Z-axis was between those of the X-axis and Y-axis, the maximum peak was found at 400 g. The relatively lower peaks were observed until 5 ms in the Y-axis. Displacement in the Z-axis can be explained by the dorsoventral motion of the skull, corresponding to up-and-down oscillations with respect to the Z-direction. This motion in the Z-axis is initiated after the first peak in the X-axis, that is, after release of the impact. Movements in each of the three-axes can contribute to processes of impact energy dissipation by dampening specific oscillations that could potentially be harmful to the brain.

The effect of the impact speeds in the X-axis at a 1, 2, and 3 m s^{-1} on the acceleration profile was studied; results are shown in Figure 3b and Figure S2, Supporting Information (see details in S1.3, Supporting Information). Due to technical limitations of the experimental setup, a 7 m s^{-1} impact speed was not tested directly. The results showed that the peak amplitude of acceleration linearly increases with higher impact speed. The pattern of the acceleration profile remains similar among the three tested speeds, while the impact duration remains unchanged. Based on the results, we can estimate the amplitude of accelerations at the impact speed of 7 m s^{-1}, which is the maximum value that has been recorded for woodpeckers. From a simple linear regression, the peak acceleration of 7 m s^{-1} can be estimated at 1000 g. By scaling it down to the real size of a woodpecker skull, we find that acceleration would reach about 6800 g for the real case (for calculation see S1.6, Supporting Information) which shows a good agreement with other reported pecking conditions (1200 g in the original scale),[3] meaning that our experimental impact testing

with 3D printed skull models can serve as a basis for comparative analyses with real life cases.

Analysis of failure of the skull models after impact testing can serve as valuable information, because in vivo testing that resulted in damage to the skull bones of living woodpeckers would not be possible without sacrificing a bird. In addition, because the 3D printed skull and beak have essentially the same material properties unlike the real bird, it allows us to analyze the sole effect of the structure specifically. Note that the black circles in Figure 3d,e indicate the tip of the beak, which was wrapped with a polylactic acid (PLA) shrinkable film to protect it from breakage during impact testing, after several trials and errors. Before wrapping with the PLA film, the printed skull models would sustain damage at the tip of the beak as shown in Figure 3c. After several tests, the same type of damage at the tip of the beak was observed repeatedly; we therefore utilized the PLA film to wrap around the tip of the beak to protect this part from breakage. By protecting the beak tip, we can observe if other structures can be damaged after impact. Breakage was mostly found to happen at the jugal bone, generally after two or three impact tests, as shown in Figure 3d. The jugal bones were the only damaged structures we found on both no overhang (top) and overhang models (bottom) highlighted with red ellipses. By performing the same test on the same sample five times, both sides of the jugal bones would completely break, while other structures would still remain intact, as shown in Figure 3e. The failure analysis of the 3D printed skull models implies that the impact energy may be dissipated at the tip of the beak and the jugal bones. The other parts of the internal skull bones were examined but remained intact after five

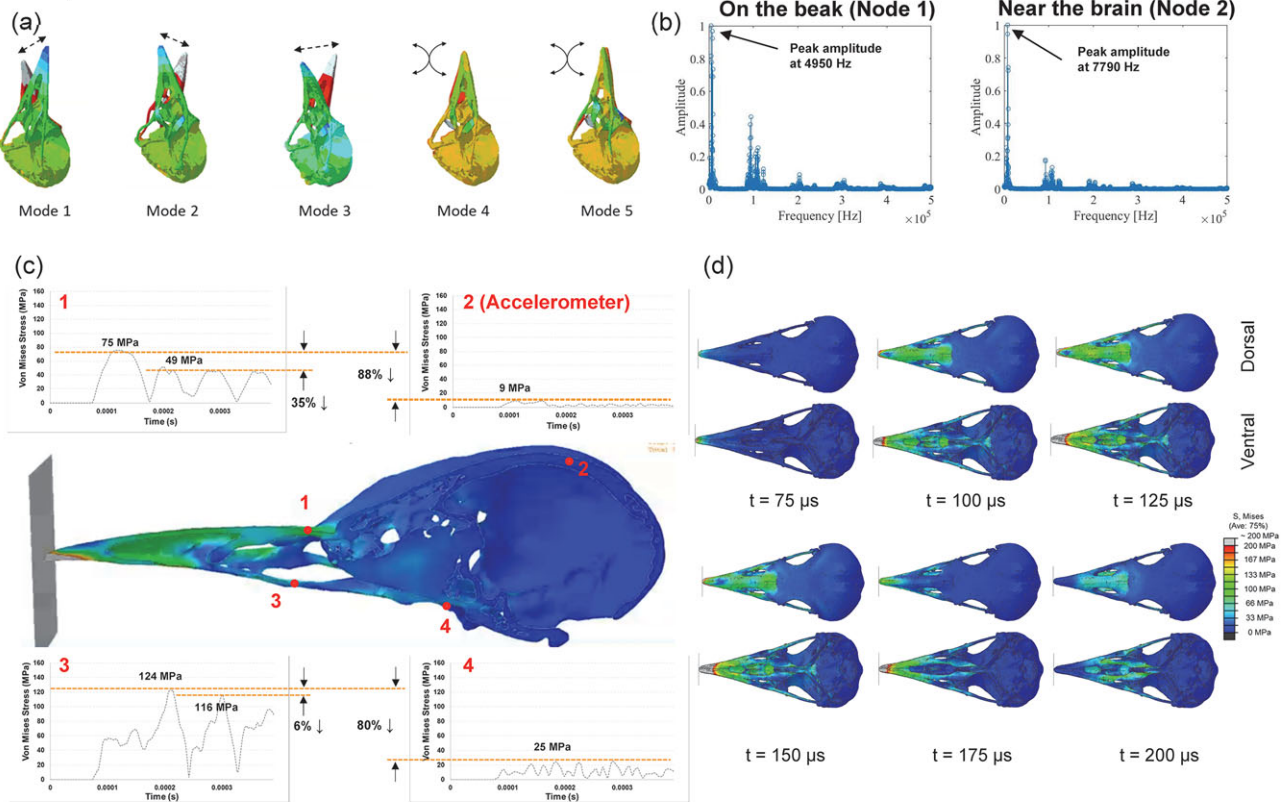## Computational results

Figure 4. Computational results of the impact testing with 3D meshed skull models. a) Five natural frequency modes associated with the vibration of the skull. b) A representative result of Ricker's pulse analyses at node 1 and 2. c) The sagittal-section view of the skull model and the plots of von Mises stress at four nodes. 1: on the upper beak bone prior to the interface between the upper beak and the frontal bone. 2: on the parietal bone near the brain (where an accelerometer was attached in the experimental setup). 3: on the palatine bone. 4: on the jugal bone. d) Time-lapse images of von Mises stress distribution on the skull bone models during the woodpecker's pecking at a 7 m s^{-1} of impact speed.

impact incidents. In nature, the tip of the beak bone is protected by the keratinized sheath (called the rhamphotheca[13]), and jugal bones, as well as other parts of the skull, are mainly surrounded by soft tissue. Nonetheless, the failure analysis allows one to identify areas that are the most sensitive to breakage in the skull.

Frequency modal analyses of the 3D printed skull model were performed to evaluate the natural frequencies of the skull bone structure. According to Laksari et al.,[17] repeated low-acceleration head impacts may cause mild brain trauma in humans, therefore, understanding the skull-brain dynamics is important. The authors reported that a low-frequency resonance between the skull and the brain in humans occurred at ≈15 Hz in an underdamped system (the system oscillates with decreasing amplitude to a convergent point) and more commonly at <20 Hz in other contact sports. This resonance can amplify the relative brain-skull motion, which is more likely to cause brain damage. In primates and humans, low-range natural frequencies (5–10 Hz) were observed for rotational brain motion.[18] However, the resonance frequencies of the skull were reported around 1000 Hz in humans during head impacts. As a boundary condition, we fixed the models at the point where the skull meets the neck, and cal-

culated the first five modes of natural frequency of the woodpecker skull model. The five calculated modes are presented in **Figure 4**a, showing the five (possible) structural free oscillations, which depend on the stiffness of the structure k (and henceforth its Young's modulus E (GPa), density ρ (Kg m^{-3}), and effective length L (m)) and its mass m (kg), as indicated by the following relationship:

$$f_n = \frac{\alpha_n}{2\pi}\sqrt{\frac{k}{m}} = \frac{\alpha_n}{2\pi}\sqrt{\frac{E\,I}{A\rho\,L^4}} \tag{1}$$

where f_n is natural frequency in hertz (cycles/second), I is the second area moment of inertia (kg·m^2), A is the equivalent cross-sectional area (m^2), L is the effective length (m), and α_n is a parameter that depends on the boundary conditions and the vibration mode.

Each mode corresponds to a specific motion at a certain excited frequency: up and down (along the Z-axis) bending motion of the skull bone for modes 1 (4790 Hz), 2 (7026 Hz), and 3 (7458 Hz) and twisted torsional motion between the palatine and jugal bones for mode 4 (8146 Hz) and 5 (10024 Hz).

**ADVANCED
SCIENCE NEWS**

www.advancedsciencenews.com

**ADVANCED
THEORY AND
SIMULATIONS**

www.advtheorysimul.com

The average frequency of the sideways motion of the 3D printed skull model, recorded with the high-speed camera, was found to be 629 Hz (see details in S1.4 and Figure S3, Supporting Information). This value, when taking into account the model relative size and the material stiffness compared to the real skull, is equivalent to 4257 Hz (see details in S1.4 and S1.6, Supporting Information) a result that can be assimilated to the first natural frequency (4790 Hz). Considering the size of the skull and brain of woodpeckers, the traumatic resonance in woodpeckers might occur at a much higher frequency range than for humans (due to a smaller mass, following the allometric relationship in Equation (1)). However, the mechanical properties of the brain of woodpeckers (e.g., stiffness (k) in Equation (1)) have never been reported; hence, an accurate calculation of the natural frequency of the woodpecker brain and followed with an assessment of the resonance frequency between the skull and the brain of woodpeckers are impossible at this time. However, we can expect that the natural frequency of the woodpecker brain should remain low (below 4000 Hz) to avoid synchronized resonance with the skull bone. This is nevertheless an interesting subject for future work, that could extend Gibson's allometry analysis.[8]

Ricker's pulse simulations and the associated frequency spectrum analyses were performed to obtain a clear visualization of excited frequencies after impact, contrary to the case of a direct impact input that can result in noisy data. As shown in Figure 4b, the dominant frequencies of the skull bone at the node 1 and node 2 appear to be around 4950 and 7790 Hz, respectively. No frequencies <4000 Hz are observed. For a comparison between two nodes on the skull bone model without the overhang, node 2 shows a peak amplitude at a higher frequency than node 1 (on the beak), implying that the structure of the skull bone is designed to be isolated from the vibration from the beak. The effect of body mass/volume on the frontal bone between two models (with and without the overhang) does not seem to show any difference in terms of calculated natural frequencies and the distribution of peak amplitude at these frequencies (Figure 4b) which seems to imply that there is no discernable effect of the frontal overhang in exciting different vibrational frequencies.

To analyze the stress wave pathway during pecking in the normal direction, a dynamic impact analysis was conducted with a 7 ms^{-1} of speed. The evolution of the von Mises stress over time after impact for the skull model is plotted in Figure 4c. The values are taken at the four specific nodes described on Figure 2c. Along the dorsal line (through nodes 1 and 2), node 1, located ahead of the frontal overhang showed the highest stress level (max peak ≈75 MPa), and then, the value dropped by 35% at the second peak. The maximum stress level decreased significantly at node 2, with a peak value 88% lower (max ≈9 MPa) than at node 1. Along the ventral line, a similar pattern can be observed; node 3 shows a higher stress level (max ≈124 MPa right after impact, then a second peak at ≈116 MPa) than node 4 (max ≈25 MPa) (see details in S1.5 and Figure S4, Supporting Information). Among all these nodes, node 3 is the one undergoing the highest stress level, implying that the four main oscillation cycles observed at every location correspond to the dorso-ventral motion of the upper beak after impact, as discussed above. Note that the general trend on the dorsal and ventral line between the two models is almost the same, the addition of body mass (in the

model) does not seem to affect the stress levels on the skull bones. However, a higher stress level was observed along the ventral line, which indicates that the pathway of the stress propagation comes from the upper beak bone to the bottom of the skull bone and the neck and eventually to the rest of body. The variation of the stress on the dorsal line seems not related to the frontal overhang sizes, but a higher level of stress on the ventral line may suggest that the morphology of the skull bone structure is beneficial to deflect the main stress wave toward the bottom part of the skull bones, rather than toward the brain. In addition, the highest stress level was found to be reached at the beak tip (gray color in Figure 4c, with values above 200 MPa), which shows a good agreement with the failure analysis of the damaged 3D printed skull models, as shown in Figure 3c.

A time-history of the stress distribution shows how the stress wave propagates through the skull bone at each time step, as shown in Figure 4d. The first impact occurrs around 75 µs, when the tip of the upper beak bone shows a change of stress level. Around 100 µs, the first stress wave reaches the caudal end of the upper beak bone and the rostral end of the frontal bone. The highest stress level in this region was observed around 125 µs, after which the stresses decrease down to zero around 200 µs. The first stress wave fully propagated along the dorsal line around 200 µs, after which a second wavefront traverses the dorsal line. On the other hand, along the ventral line, the first stress wave reaches its peak at node 3 at 100 µs and at node 4 at 150 µs, respectively. Overall, a notable fact is that the stresses remain at a relatively lower level (≈9 MPa, as shown in Figure 4c(2),d) near the brain-case during the propagation of the first shockwave, that is, until 200 µs. As a result of the stress analysis, it is found that there are no notable differences between the two skull models, either with or without a frontal overhang. This implies that the natural structure of woodpecker's skull bone was designed to minimize the stress propagation from the upper beak to the brain-case, which can intrinsically serve as a mechanism to protect its brain.

4. Conclusion

To confirm the structural differences on the skull bone structure in woodpeckers, µ-CT was utilized to investigate 3D shape between two species: white-headed and golden-fronted woodpeckers. Based on the biologist's observation according to Smith, we hypothesized that the anatomical differences on the skull bone can be affected by the different food sources and the different pecking habits, so as to have a better mechanical function against mechanical impact or shock. To test this hypothesis, a 3D mesh model of a golden-fronted woodpecker was developed and an artificial overhang feature was added on the model, mimicking the white-headed woodpecker skull bone, to assess its potential benefit in brain protection. An experimental test with a customized drop weight impact testing tower with 3D printed plastic skulls, as well as dynamic FEA, were conducted for each model to obtain acceleration versus time curves, observe failure modes of impacted 3D printed skull models, identify natural frequencies, and record the free vibrations of the structures after impact with frequency spectral analyses, and determine von Mises stress levels at each predefined node. The main findings are:

**ADVANCED
SCIENCE NEWS**

www.advancedsciencenews.com

**ADVANCED
THEORY AND
SIMULATIONS**

www.advtheorysimul.com

- A drop tower impact testing setup using 3D printed skull models showed the peak accelerations in the X-axis as the main impact direction. A vibrational motion along the Z-axis was found, indicating a dorsoventral motion of the whole skull model.

- From the 3D printed skull models, failure analysis showed that the beak tip and the jugal bones are the mainly damaged structures during dynamic impact.

- Natural frequency and Ricker's pulse analysis showed that the five representative natural frequency modes correspond to two different vibrational motions: the dorsoventral motion of the skull bone and the twisted torsional motion between the palatine and jugal bones. After pulsed impact, a higher resonance frequency was found on the skull bone near the brain than on the beak bone. While using frequency mismatch is a common practice in structural engineering, this result is a good example of bioinspired frequency control attained through the modification of only geometrical parameters and can be applied to a design strategy for protective head gears in contact sports. Further characterization of other anatomical features and their contribution with impact mitigation may also help deepen understanding of this bioinspired approach.

- von Mises stress analysis showed that the main stress wavefront from the impact at the beak tip propagated through the ventral line (the jugal bones) of the head toward the neck/spine. The von Mises stress level near the brain remained at a significantly lower level than the rest of the skull bone structure.

- Without sacrificing a living animal, we were able to test our hypothesis and answer the question: What is the structural role and benefit from the frontal overhang on the skull bone of woodpeckers? Although the effect of the frontal overhang on vibrational motion was negligible, we found that, more importantly, the skull bone is naturally designed to limit the stress wavefront toward the body rather than the braincase during pecking.

- Both 3D printed skulls and computational models developed in this study can be used to further identify and assess a dynamic interaction between the skull and brain (i.e., using a gel-like brain surrogate material) in woodpeckers to represent a nontraumatic brain injury animal model, as a future direction of this study.

5. Future Work

- Through this manuscript, an isotropic, continuous, and homogeneous 3D printed model was implemented, which provides a better, simpler understanding of the isolated anatomical features solely. However, a natural bone has a hierarchical structure with different materials forming an organic-inorganic composite; the energy absorption mechanism is thus different from our 3D printed beak-skull models. In order to mimic the natural bone and analyze the impact resistance of the real beak-skull bones, a composite structure combined with organic and inorganic materials can be printed out together through an advanced 3D printing technique as one of our future goals.

- In addition, we have performed a failure analysis of the 3D printed skull models in micro scale, but a micro scale damage analysis is worth investigating when considering some printing conditions, such as a curing, orientation of material stacking, and adhesion/tearing forces between two materials if we can print multiple materials simultaneously. This work can be our next step in failure analysis using different 3D printing configurations against mechanical impact, as we are also attempting to avoid testing on actual biological samples.

- The effect of a hinge opening angle (α) between the frontal bone and the beak bone (earlier mentioned in Introduction) was found to be negligible. The relationship between the hinge opening angle and the level of stress propagated through the beak and skull bone models in relation to reported pecking habits will be an interesting topic to examine, although the angle was only used to quantify the main structural difference between two woodpecker species to focus on whether the presence of the frontal overhang or not in this manuscript.

- Our approach to build two comparative skull models is started as we add up the artificial frontal overhang on the skull of the non-overhang species (golden-fronted woodpecker); however, the alternative method to artificially remove the frontal overhang structure on the skull of the overhang species (white-headed woodpecker) can be an interesting approach for comparison.

6. Experimental Section

μ-CT: An acorn woodpecker (*Melanerpes formicivorus*) was scanned by μ-CT (SkyScan 1076, Bruker microCT, Konich, Belgium) in the previous paper.[19] Raw data of three other woodpeckers, an ivory-billed woodpecker (*Campephilus principalis*), a white-headed woodpecker (*Picoides albolarvatus*), and a golden-fronted woodpecker (*Melanerpes aurifrons*) were obtained from digimorph.org operated by High-Resolution X-ray CT Facility at the University of Texas, Austin. Each skull bone was visualized and analyzed using Amira software (FEI Visualization Sciences Group, Burlington, MA). After verifying the 3D volume rendering models for each skull, an image segmentation process was carried out based on X-ray intensity to generate a 3D mesh model of the skull bone.

Mesh Model Generation for Simulation and 3D Printing: GeoMagic (3D Systems, Morrisville, NC) and GMSH software[20] were used to fix triangulation errors obtained from the initial reconstruction with Amira and to generate the solid FE meshes.

3D Printing of Skull Models and Impact Testing: The woodpecker skull models were printed out using a 3D printer (Object 350 connex3, Stratasys, Eden Prairie, MN). A VeroClear material (Young's modulus: 2–3 GPa, density: 1.20–1.30 g cm^{-3}, transparent material) was used to print the skull bone models. A custom-built drop weight test tower was used to simulate the impact of the beak and skull bones, a detailed description of dimensions and specifications can be found in the previous work.[21]

Dynamic FEA: Dynamic FEA of an impact event between the woodpecker skull and a rigid solid plate was carried out on a commercially available software (Abaqus/Explicit). The skull was slightly rotated to align the main axis of the beak, calculated by finding the best fitting plane of symmetry, with the direction of pecking.

Frequency Modal Analysis: Frequency modal analyses of the two models were performed to identify the natural modes of vibration, and to evaluate the effects of the added mass and volume on the natural frequencies of the woodpecker skull due to the added overhang. Subsequently, dynamic impact cases with a Ricker Pulse input, along the direction of pecking at the tip of the beak, were simulated. The Ricker pulse produces an impact with a known spectrum, and results in a clearer acceleration profile of the structure in the frequency domain.

[1] National Center for Injury Prevention and Control. *Steps to Prevent a Serious Public Health Problem*; Report to Congress on Mild Traumatic Brain Injury in the United State; Technical Report; Centers for Disease Control and Prevention: Atlanta, GA **2003**, pp. 1–7.

[2] A. C. McKee, R. C. Cantu, C. J. Nowinski, E. T. Hedley-Whyte, B. E. Gavett, A. E. Budson, V. E. Santini, H.-S. Lee, C. A. Kubilus, R. A. Stern, *J. Neuropathol. Exp. Neurol.* **2009**, *68*, 709.

[3] a) P. A. May, J. Fuster, P. Newman, A. Hirschman, *Lancet* **1976**, *307*, 1347; b) P. A. May, J. M. Fuster, J. Haber, A. Hirschman, *Arch. Neurol.* **1979**, *36*, 370.

[4] W. J. Bock, *J. Morphol.* **1964**, *114*, 1.

[5] W. H. Burt, *Adaptive Modifications in the Woodpeckers*, University of California Press, Berkeley, California **1930**.

[6] F. E. L. Beal, *Food of the Woodpeckers of the United States*, U.S. Department of Agriculture, Washington D.C. **1911**.

[7] a) C. K. Virginia, *Auk* **1980**, *97*, 521; b) D. L. Leonard, J. A. Heath, *J. Ornithol.* **2010**, *151*, 771.

[8] L. J. Gibson, *J. Zool.* **2006**, *270*, 462.

[9] J. Oda, J. Sakamoto, K. Sakano, *JSME Int. J., Ser. A* **2006**, *49*, 390.

[10] P. Zhou, X. Q. Kong, C. W. Wu, Z. Chen, *J. Bionic Eng.* **2009**, *6*, 214.

[11] a) L. Wang, J. T.-M. Cheung, F. Pu, D. Li, M. Zhang, Y. Fan, *PLoS One* **2011**, *6*, e26490; b) Z. Zhu, W. Zhang, C. Wu, *Sci. China Technol. Sci.* **2014**, *57*, 1269; c) Z. Zhu, C. Wu, W. Zhang, *J. Bionic Eng.* **2014**, *11*, 282; d) Y. Liu, X. Qiu, X. Zhang, T. X. Yu, *PLoS One* **2015**, *10*, e0122677.

[12] S.-H. Yoon, S. Park, *Bioinspiration Biomimetics* **2011**, *6*, 016003.

[13] J.-Y. Jung, A. Pissarenko, N. Yaraghi, S. Naleway, D. Kisailus, M. Meyers, J. McKittrick, *J. Mech. Behav. Biomed. Mater.* **2018**, *84*, 273.

[14] W. J. Bock, *Ostrich* **1999**, *70*, 23.

[15] J. Hanken, B. K. Hall, *The Skull, Volume 3: Functional and Evolutionary Mechanisms*, University of Chicago Press, Chicago, Illinois **1993**.

[16] a) H. Ryan, *CSEG Recorder* **1994**, *19*, 8; b) D. Restrepo, Doctoral Dissertation, Purdue University, **2015**; c) Y. Wang, *Geophys. J. Int.* **2015**, *200*, 111.

[17] K. Laksari, L. C. Wu, M. Kurt, C. Kuo, D. C. Camarillo, *J. R. Soc., Interface* **2015**, *12*, 20150331.

[18] A. E. Hirsch, A. K. Ommaya, R. M. Mahone, *Tolerance of Subhuman Primate Brain to Cerebral Concussion*, Naval Ship Research and Development Center, Washington D.C. **1968**.

[19] J.-Y. Jung, S. E. Naleway, N. A. Yaraghi, S. Herrera, V. R. Sherman, E. A. Bushong, M. H. Ellisman, D. Kisailus, J. McKittrick, *Acta Biomater.* **2016**, *37*, 1.

[20] C. Geuzaine, J.-F. Remacle, *Int. J. Numer. Methods Eng.* **2009**, *79*, 1309.

[21] S. Lee, E. E. Novitskaya, B. Reynante, J. Vasquez, R. Urbaniak, T. Takahashi, E. Woolley, L. Tombolato, P. Y. Chen, J. McKittrick, *Mater. Sci. Eng., C* **2011**, *31*, 730.

[22] W. J. Bock, *Neth. J. Zool.* **1999**, *49*, 45.